Macroeconomic Dynamics, **22**, 2018, 1555–1583. Printed in the United States of America.
doi:10.1017/S1365100516000821

A COMPARISON OF NUMERICAL METHODS FOR THE SOLUTION OF CONTINUOUS-TIME DSGE MODELS

Juan Carlos Parra-Alvarez
Aarhus University and CREATES

This study evaluates the accuracy of a set of techniques that approximate the solution of continuous-time Dynamic Stochastic General Equilibrium models. Using the neoclassical growth model, I compare linear-quadratic, perturbation, and projection methods. All techniques are applied to the Hamilton–Jacobi–Bellman equation and the optimality conditions that define the general equilibrium of the economy. Two cases are studied depending on whether a closed-form solution is available. I also analyze how different degrees of non-linearities affect the approximated solution. The results encourage the use of perturbations for reasonable values of the structural parameters of the model and suggest the use of projection methods when a high degree of accuracy is required.

Keywords: Continuous-Time DSGE Models, Linear-Quadratic Approximation, Perturbation Method, Projection Method

1. INTRODUCTION

During the last 20 years macroeconomy has experienced a convergence in methodology to what is known today as Dynamic Stochastic General Equilibrium (DSGE) models [see Blanchard (2009)]. In general, it is not possible to derive analytical solutions for the policy functions that describe the equilibrium outcomes of these models. Economists have restored to numerical methods that differ in accuracy and computational costs to approximate these unknown functions. The differences across methods were initially studied in Taylor and Uhlig (1990) and later on in Aruoba et al. (2006) for discrete-time economies. However, little attention has been paid in this regard to structural stochastic dynamic models in continuous-time. This paper attempts to fill this gap in the literature, and therefore, it complements

I would like to thank the editor and two anonymous referees for extremely useful comments and suggestions, as well as the participants of the 18th Annual Conference on Computing in Economics and Finance in Prague, the 6th CSDA International Conference on Computational and Financial Econometrics in Oviedo and the CDMA Workshop on DSGE models in St. Andrews for their helpful comments. I would also like to thank Olaf Posch, Bent Jesper Christensen, Jesús Fernández-Villaverde, Kenneth Judd, Martin Møller Andreasen, Willi Semmler and seminar participants at CREATES for useful suggestions and insights. CREATES (Center for Research in Econometric Analysis of Time Series) is funded by the Danish National Research Foundation. Address correspondence to: Juan Carlos Parra-Alvarez, Department of Economics and Business Economics, Fuglesangs Allé 4, 8210 Aarhus V, Denmark; e-mail: jparra@econ.au.dk.

 1365-1005/17

previous works by Judd (1996), Gaspar and Judd (1997), Judd (1998), Miranda and Fackler (2002), Kompas and Chu (2012), and Posch and Trimborn (2013).

Macroeconomic models in continuous-time exhibit some theoretical and computational features that make it, in some cases, more attractive than their discrete-time counterpart. They are sometimes preferred because of their analytical tractability. In fact, it is possible to derive closed-form solutions for a wider class of models without the need for strong parametric restrictions. In addition, since the decision interval of the model is not tied to the observation interval in the data, continuous-time models do not impose a priori a perfect synchronization of decisions among economic agents. They also allow for a clear distinction between flows and stocks in the economy as shown for example in Bergstrom (1984) and Harvey and Stock (1989). Continuous-time methods have also become popular in macro-finance since they provide a simple and tractable framework to integrate asset pricing theories studied in the finance literature to the real side of the economy. Examples of the potential benefits of continuous-time macro-finance models include Brennan (1998), Grinols and Turnovsky (1993), Xia (2001), Posch (2011), Wachter (2013), among many others. Finally, continuous-time methods are also well-suited to study situations where actions are taken infrequently because they entail a fixed cost [“impulse control" problems as described in Stokey (2009)]. For instance, the decision of a country to default on its sovereign debt under different monetary policy regimes can be analyzed using these techniques, as in Nuño and Thomas (2015).

From a computational perspective, continuous-time models are a promising tool to the extent that the optimality conditions that describe the equilibrium allocations of a stochastic economy are deterministic [Chang (2009)]. Therefore, there is no need to approximate expected values, and hence, the computational cost and the numerical errors can be reduced. As shown in Doraszelski and Judd (2012), the continuous-time framework also reduces the curse of dimensionality given that the dynamic programming equation does not include any composition of functions or expectation operators. However, these advantages come at a small cost as now the problem requires the approximations of the second-order derivatives of the value function.

The purpose of this paper is to assess the performance of different numerical methods to compute an approximated solution of continuous-time DSGE models based on the maximized Hamilton–Jacobi–Bellman (HJB) equation and the first-order conditions that describe the general equilibrium of the economy. In particular, I compare the results obtained from using (i) linear-quadratic (LQ) approximations; (ii) first- and second-order perturbations; and (iii) projection methods. Despite being all well-known procedures, little is known about their relative performance. The methods are evaluated in terms of accuracy and computing time when applied to a continuous-time version of the stochastic neoclassical growth model with endogenous labor studied in Aruoba et al. (2006). Under a suitable parameterization, the model admits a closed-form solution that can be used to assess the different approximations.[1] The robustness of the methods is checked by

https://doi.org/10.1017/S1365100516000821 Published online by Cambridge University Press

using alternative calibrations that differ in the degree of non-linearities introduced into the model.

Three main results are obtained from this exercise. First, I find that despite their conceptual and computational differences, all methods provide an acceptable degree of accuracy around the deterministic steady state. This result is robust to different values of the volatility of the exogenous processes as long as the risk aversion parameter is not unreasonably high. Outside the deterministic steady state, projection methods are the most reliable and stable, although highly dependent on a good initial guess.

Second, despite perturbation being only locally accurate, the increase in the order of approximation, which can be done at a low additional computational cost, improves substantially the goodness of fit. However, as mentioned in Den Haan and De Wind (2010) and Aldrich and Kung (2010), some caution is needed when relying in the virtues of perturbation since Taylor approximations are only accurate within a radius of convergence around the point of approximation. Hence, if the grid of the state variables includes values that lie outside this radius of convergence, a local approximation can deteriorate rapidly regardless of its order.

Third, LQ approximations are usually less accurate than perturbation methods despite both of them using the same local information to build the approximation. When the method is applied to models with linearized constraints, the policy functions are incorrectly approximated outside the deterministic steady state. However, if the constraints are linear by construction, the optimal policies are correctly approximated for a given radius of convergence. Such a distinction does not affect the approximation of the value function.

Similar to the recommendations of Aruoba et al. (2006) for discrete-time models, the results obtained in this paper should stimulate the use of perturbation methods, preferably with orders of approximation higher than one, and suggest relying on projection techniques whenever high accuracy and stability are needed.

The rest of the paper is organized as follows. Section 2 describes the general stochastic control problem and summarizes the different methods used to approximate its solution. Section 3 presents the benchmark model that will be used to test the different numerical techniques and establishes the conditions under which a closed-form solution exists. Section 4 reports the numerical results and accuracy measures obtained under different setups and calibrations, and presents a brief discussion on computing time. Finally, Section 5 concludes.

2. GENERAL PROBLEM AND SOLUTION METHODS

Let $(\Omega, \mathcal{F}, P)$ be a filtered probability space with filtration $\{\mathcal{F}_t\}$, $\mathbf{s}_t \in \mathbf{S} \subset \mathbf{R}_+^m$ an m-dimensional vector of predetermined endogenous and exogenous state variables at time t with right-continuous sample paths, left-hand limit, and initial value $\mathbf{s}_0$, and $\mathbf{c}_t \in \mathcal{D}(\mathbf{S}) \subset \mathbf{R}_+^n$ an n-dimensional vector of non-negative endogenous-control variables at time t whose coordinates are functions of the state variables. The set $\mathcal{D}(\mathbf{S})$ denotes the set of admissible controls. The evolution of the state

https://doi.org/10.1017/S1365100516000821 Published online by Cambridge University Press

vector is given by the autonomous controlled diffusion process:

$$\mathrm{d}\mathbf{s}_t = \mu\left(\mathbf{s}_t, \mathbf{c}_t\right)\mathrm{d}t + \Sigma^{1/2}\left(\mathbf{s}_t, \mathbf{c}_t\right)\mathrm{d}\mathbf{B}_t, \tag{1}$$

where $\mu(\mathbf{s}_t, \mathbf{c}_t) \in \mathbf{R}^m$ and $\Sigma^{1/2}(\mathbf{s}_t, \mathbf{c}_t) \in \mathbf{R}^{mp}$ are the real-valued drift vector Lipschitzian function and real-valued square root variance–covariance matrix Lipschitzian function, respectively. $\mathbf{B}_t$ is a p-dimensional vector of standard Brownian motions representing stochastic disturbances that affect the state variables. Define $\Sigma(\mathbf{s}_t, \mathbf{c}_t) = \Sigma^{1/2}(\mathbf{s}_t, \mathbf{c}_t)\Sigma^{1/2}(\mathbf{s}_t, \mathbf{c}_t)' \in \mathbf{R}^{mp}$ to be the variance–covariance matrix of those disturbances.

The decision problem of the agent corresponds to the autonomous discounted stochastic optimal control problem:

$$V\left(\mathbf{s}_0\right) = \max_{\{\mathbf{c}_t\}_{t=0}^{\infty} \in \mathcal{D}(\mathbf{s}_t)} \mathbf{E}_0 \int_0^{\infty} e^{-\rho t}\pi\left(\mathbf{s}_t, \mathbf{c}_t\right)\mathrm{d}t,$$

subject to equation (1) and $\mathbf{s}_0$ given, where $\mathbf{E}_0$ denotes the expectation operator conditional on the information available at time $t = 0$, $\rho > 0$ is a constant discount factor, and $\pi(\mathbf{s}_t, \mathbf{c}_t) \in \mathbf{R}$ is the time-homogeneous, continuous, and integrable objective function. For simplicity, it is assumed that the variance–covariance matrix of the disturbances is control independent. The function $V(\mathbf{s}_0) \in \mathbf{R}$ denotes the maximum expected value, or value function, obtained at $t = 0$ when $\mathbf{s} = \mathbf{s}_0$.

A necessary condition for optimality is given by the HJB equation[2]:

$$0 = \max_{\mathbf{c}_t \in \mathcal{D}(\mathbf{s}_t)} \left\{\pi\left(\mathbf{s}_t, \mathbf{c}_t\right) - \rho V\left(\mathbf{s}_t\right) + \mu\left(\mathbf{s}_t, \mathbf{c}_t\right)\nabla V\left(\mathbf{s}_t\right) + \frac{1}{2}\mathrm{trace}\left(\Sigma\left(\mathbf{s}_t\right)\nabla^2 V\left(\mathbf{s}_t\right)\right)\right\}, \tag{2}$$

where $\nabla V(\mathbf{s}_t)$ is the gradient of the value function and $\nabla^2 V(\mathbf{s}_t)$ is the associated Hessian matrix.

The first-order conditions for any interior solution are:

$$\pi_c\left(\mathbf{s}_t, \mathbf{c}_t\right) + \mu_c\left(\mathbf{s}_t, \mathbf{c}_t\right)\nabla V\left(\mathbf{s}_t\right) = 0, \tag{3}$$

for each $c_t \in \mathbf{c}_t$, which implicitly makes the vector of controls a function of the state vector, $\mathbf{c}_t = \mathcal{P}(\mathbf{s}_t)$. The vector function $\mathcal{P} : \mathbf{R}^m \to \mathcal{D}(\mathbf{s}_t)$ maps every possible value of the state vector at time t into the optimal control vector. The implicit maximized (concentrated) HJB equation reads as follows:

$$0 = \pi\left(\mathbf{s}_t, \mathcal{P}\left(\mathbf{s}_t\right)\right) - \rho V\left(\mathbf{s}_t\right) + \mu\left(\mathbf{s}_t, \mathcal{P}\left(\mathbf{s}_t\right)\right)\nabla V\left(\mathbf{s}_t\right) + \frac{1}{2}\mathrm{trace}\left(\Sigma\left(\mathbf{s}_t\right)\nabla^2 V\left(\mathbf{s}_t\right)\right), \tag{4}$$

which together with the first-order conditions determines the unknown functions $V(\mathbf{s}_t)$ and $\mathcal{P}(\mathbf{s}_t)$ and forms the basis for all the numerical procedures to be introduced later. A solution to the stochastic optimal control problem amounts to finding these unknown functions such that they solve the continuum of problems

https://doi.org/10.1017/S1365100516000821 Published online by Cambridge University Press

described by equation (2). The mapping $\mathcal{P}$ is called policy function and represents the optimal response of agents to a given set of state values.

In general, a solution to this problem can not be found analytically, and it is necessary to use numerical methods to approximate it. In the following subsections, I briefly introduce different methods to numerically solve continuous-time stochastic optimal control problems. In particular, I use LQ approximations, perturbations, and projection methods. Alternative techniques can be found in Tapiero and Sulem (1994), Candler (2004), Posch and Trimborn (2013), and Achdou et al. (2014). For a detailed explanation of each of the techniques I refer the reader to the reference list.

2.1. Linear-Quadratic Approximation

LQ approximation uses local information to replace the original non-linear stochastic optimal control problem with a more tractable problem for which a solution can be easily found. In fact, it can be shown that the resulting policy functions are linear in the state variables. LQ approximations have been extensively used in economics. The first attempts to apply this technique in the field can be found in Magill (1977a) for deterministic models and in Magill (1977b) for stochastic models, even though the method only became popular after the seminal paper of Kydland and Prescott (1982). Further developments and implementation alternatives can be found in Anderson et al. (1996).

Formally, let $\hat{\mathbf{s}}_t = (\mathbf{s}_t - \mathbf{s}^{ss})$ and $\hat{\mathbf{c}}_t = (\mathbf{c}_t - \mathbf{c}^{ss})$ denote the absolute deviations of the state and control variables from their deterministic steady-state values, respectively. The LQ method approximates the original non-linear problem in $(\hat{\mathbf{s}}_t, \hat{\mathbf{c}}_t)$ by constructing a second-order Taylor expansion of the objective function, $\pi(\mathbf{s}_t, \mathbf{c}_t)$, and a first-order Taylor expansion of equation (1) around the deterministic steady state of the model. The LQ stochastic control problem is given by:

$$V(\hat{\mathbf{s}}_0) = \max_{\{\hat{\mathbf{c}}_t\}_{t=0}^{\infty} \in \mathcal{D}(\hat{\mathbf{s}}_t)} \mathbf{E}_0 \int_0^{\infty} e^{-\rho t} \left(\hat{\mathbf{s}}_t' \mathbf{R} \hat{\mathbf{s}}_t + \hat{\mathbf{c}}_t' \mathbf{Q} \hat{\mathbf{c}}_t + 2\hat{\mathbf{c}}_t' \mathbf{W}' \hat{\mathbf{s}}_t \right) \mathrm{d}t,$$

subject to:

$$\mathrm{d}\hat{\mathbf{s}}_t = [\mu_{\mathbf{s}}(\mathbf{s}^{ss}, \mathbf{c}^{ss})\hat{\mathbf{s}}_t + \mu_{\mathbf{c}}(\mathbf{s}^{ss}, \mathbf{c}^{ss})\hat{\mathbf{c}}_t]\mathrm{d}t + \Sigma^{1/2}(\mathbf{s}^{ss})\mathrm{d}\mathbf{B}_t,$$

where now $\hat{\mathbf{s}}_t$ is an $(1+m)\times 1$ vector with the first element being the constant 1. The matrices $\mu_{\mathbf{s}}(\mathbf{s}^{ss}, \mathbf{c}^{ss})$, $\mu_{\mathbf{c}}(\mathbf{s}^{ss}, \mathbf{c}^{ss})$, and $\Sigma^{1/2}(\mathbf{s}^{ss})$ are of dimensions $(1+m)\times(1+m)$, $(1+m)\times n$, and $(1+m)\times p$ respectively with the elements of their first rows all equal to zero. Furthermore, $\mathbf{R}$, $\mathbf{Q}$, and $\mathbf{W}$ are the $(1+m)\times(1+m)$, $n\times n$, and $(1+m)\times n$ matrices resulting from the second-order Taylor expansion of $\pi(\mathbf{s}_t, \mathbf{c}_t)$, respectively. A detailed derivation of their components can be found in McCandless (2008).

https://doi.org/10.1017/S1365100516000821 Published online by Cambridge University Press

Following Ljungqvist and Sargent (2004), I introduce an equivalent problem without cross-products between the states and controls. The transformed LQ stochastic control problem becomes:

$$V\left(\hat{\mathbf{s}}_0\right) = \max_{\{\hat{\mathbf{c}}_t\}_{t=0}^{\infty} \in \mathcal{D}(\hat{\mathbf{s}}_t)} \mathbf{E}_0 \int_0^{\infty} e^{-\rho t} \left(\hat{\mathbf{s}}_t' \bar{\mathbf{R}} \hat{\mathbf{s}}_t + \hat{\mathbf{c}}_t^{\star'} \mathbf{Q} \hat{\mathbf{c}}_t^{\star}\right) \mathrm{d}t,$$

subject to:

$$\mathrm{d}\hat{\mathbf{s}}_t = \left[\bar{\mu}_{\mathbf{s}}\left(\mathbf{s}^{ss}, \mathbf{c}^{ss}\right) \hat{\mathbf{s}}_t + \mu_{\mathbf{c}}\left(\mathbf{s}^{ss}, \mathbf{c}^{ss}\right) \hat{\mathbf{c}}_t^{\star}\right] \mathrm{d}t + \Sigma^{1/2}\left(\mathbf{s}^{ss}\right) \mathrm{d}\mathbf{B}_t,$$

with $\bar{\mathbf{R}} = \mathbf{R} - \mathbf{W}\mathbf{Q}^{-1}\mathbf{W}'$ and $\bar{\mu}_{\mathbf{s}}(\mathbf{s}^{ss}, \mathbf{c}^{ss}) = \mu_{\mathbf{s}}(\mathbf{s}^{ss}, \mathbf{c}^{ss}) - \mu_{\mathbf{c}}(\mathbf{s}^{ss}, \mathbf{c}^{ss})\mathbf{Q}^{-1}\mathbf{W}'$, and where the new control vector $\hat{\mathbf{c}}_t^{\star}$ is related to the original control $\hat{\mathbf{c}}_t$ by $\hat{\mathbf{c}}_t^{\star} = \mathbf{Q}^{-1}\mathbf{W}'\hat{\mathbf{s}}_t + \hat{\mathbf{c}}_t$.

The associated HJB equation for the transformed LQ problem is given by:

$$0 = \max_{\{\hat{\mathbf{c}}_t^{\star}\}_{t=0}^{\infty} \in \mathcal{D}(\hat{\mathbf{s}}_t)} \left\{ \left(\hat{\mathbf{s}}_t' \bar{\mathbf{R}} \hat{\mathbf{s}}_t + \hat{\mathbf{c}}_t^{\star'} \mathbf{Q} \hat{\mathbf{c}}_t^{\star}\right) - \rho V\left(\hat{\mathbf{s}}_t\right) + \left(\bar{\mu}_{\mathbf{s}}\left(\mathbf{s}^{ss}, \mathbf{c}^{ss}\right) \hat{\mathbf{s}}_t \right.\right.$$
$$\left.\left. + \mu_{\mathbf{c}}\left(\mathbf{s}^{ss}, \mathbf{c}^{ss}\right) \hat{\mathbf{c}}_t^{\star}\right) \nabla V\left(\hat{\mathbf{s}}_t\right) + \frac{1}{2} \mathrm{trace}\left(\Sigma\left(\mathbf{s}^{ss}\right) \nabla^2 V\left(\hat{\mathbf{s}}_t\right)\right) \right\},$$

where the first-order conditions for any interior solution are:

$$\hat{\mathbf{c}}_t^{\star} = -\frac{1}{2}\mathbf{Q}^{-1}\left[\mu_{\mathbf{c}}\left(\mathbf{s}^{ss}, \mathbf{c}^{ss}\right)' \nabla V\left(\hat{\mathbf{s}}_t\right)'\right],$$

i.e., the controls are linear in the co-state variables, $\nabla V(\hat{\mathbf{s}}_t)$.

Let $\tilde{V}(\mathbf{s}_t)$ and $\tilde{\mathcal{P}}(\mathbf{s}_t)$ denote the approximated value and policy functions. Using a *guess-and-verify* method, it can be shown that the optimal policy functions for the LQ problem are given by:

$$\tilde{\mathcal{P}}\left(\mathbf{s}_t\right) = \mathbf{c}^{ss} - \mathbf{Q}^{-1}\left[\mathbf{W}' + \mu_{\mathbf{c}}\left(\mathbf{s}^{ss}, \mathbf{c}^{ss}\right)' \Lambda_1\right] \hat{\mathbf{s}}_t,$$

with associated value function:

$$\tilde{V}\left(\hat{\mathbf{s}}_t\right) = \Lambda_0 + \hat{\mathbf{s}}_t' \Lambda_1 \hat{\mathbf{s}}_t,$$

where Λ_1 is the solution to the continuous-time algebraic Riccati equation:

$$0 = \left[\bar{\mu}_{\mathbf{s}}\left(\mathbf{s}^{ss}, \mathbf{c}^{ss}\right)' - \frac{\rho}{2}\mathbf{I}_{m+1}\right] \Lambda_1 + \Lambda_1 \left[\bar{\mu}_{\mathbf{s}}\left(\mathbf{s}^{ss}, \mathbf{c}^{ss}\right) - \frac{\rho}{2}\mathbf{I}_{m+1}\right]$$
$$- \left[\Lambda_1 \mu_{\mathbf{c}}\left(\mathbf{s}^{ss}, \mathbf{c}^{ss}\right)\right] \mathbf{Q}^{-1}\left[\mu_{\mathbf{c}}\left(\mathbf{s}^{ss}, \mathbf{c}^{ss}\right)' \Lambda_1\right] + \bar{\mathbf{R}},$$

with $\mathbf{I}_{m+1}$ and $(m+1)$ identity matrix, and:

$$\Lambda_0 = \frac{1}{\rho} \mathrm{trace}\left(\Sigma\left(\mathbf{s}^{ss}\right) \Lambda_1\right).$$

https://doi.org/10.1017/S1365100516000821 Published online by Cambridge University Press

An undesirable property of the LQ approximation is the imposition of the certainty equivalence property on the optimal policy function for stochastic models. In particular note that $\mathbf{c}_t$ is unaffected by Λ_0, the only parameter that depends on the stochastic assumptions made on the exogenous forces that drive the economy.

Moreover, the LQ method delivers slope coefficients of the approximated policy function that are significantly different from the true coefficients whenever the constraints of the optimization problem are non-linear, and thus linearized by means of a first-order Taylor expansion. This issue, usually referred to as the "naive" LQ approximation, was initially pointed out in Judd (1998) and more recently studied in Benigno and Woodford (2012). The divergence in the approximated coefficients emerges as no information about the curvature of the state processes is included in the approximation of the objective function.

One way to overcome this inaccuracy is by reformulating the original non-linear stochastic control problem in such a way that the state processes are linear. Depending on the model at hand, this can be achieved by substituting the restrictions of the problem into the objective function and using some linear non-stochastic relations, e.g., market clearing or national account identities, to redefine the drift of the state variables [see Kydland and Prescott (1982)].

2.2. Perturbation Method

The perturbation method approximates the true value and policy functions by means of the implicit function theorem and the Taylor series expansion theorem. The outcome will be a polynomial that approximates the true solution in a neighborhood of a known solution. Following Judd (1998) and Kimball (2014), the perturbation method can be summarized by the following simple steps:

1. Express problems (2) and (3) as a continuum of problems parameterized by the added perturbation parameter ϵ with the solution for the case $\epsilon = 0$ known.
2. Differentiate the continuum of problems with respect to the control variables, $\mathbf{c}_t$, the state variables, $\mathbf{s}_t$, and the perturbation parameter, ϵ. Where possible use the envelope condition to simplify the resulting system of equations.
3. Solve for the implicitly defined derivatives at $\mathbf{s}_t = \mathbf{s}^0$ and $\epsilon = 0$, where $\mathbf{s}^0$ denotes the vector of approximation points. For the benchmark model studied in Section 3, the approximation is made around the deterministic steady state, $\mathbf{s}^0 = \mathbf{s}^{ss}$, and the associated deterministic model, $\epsilon = 0$.
4. Compute the desired order of approximation by means of Taylor's theorem and set $\epsilon = 1$. In general, the order of approximation should be determined by the first non-trivial term or dominant term, that is, apply a Taylor approximation until the first zero term is reached.

Formally, the autonomous diffusion process in equation (1) is extended with the new parameter ϵ that measures the amount of variance in the model:

$$\mathrm{d}\mathbf{s}_t = \mu\left(\mathbf{s}_t, \mathbf{c}_t\right)\mathrm{d}t + \sqrt{\epsilon}\Sigma^{1/2}\left(\mathbf{s}_t\right)\mathrm{d}\mathbf{B}_t,$$

https://doi.org/10.1017/S1365100516000821 Published online by Cambridge University Press

and hence, the "perturbed" maximized HJB equation and first-order conditions are given by:

$$0 = \pi\left(\mathbf{s}_t, \mathcal{P}\left(\mathbf{s}_t, \epsilon\right)\right) - \rho V\left(\mathbf{s}_t, \epsilon\right) + \mu\left(\mathbf{s}_t, \mathcal{P}\left(\mathbf{s}_t, \epsilon\right)\right) \nabla V\left(\mathbf{s}_t, \epsilon\right) + \frac{1}{2}\epsilon \text{ trace}\left(\Sigma\left(\mathbf{s}_t\right) \nabla^2 V\left(\mathbf{s}_t, \epsilon\right)\right),$$

and

$$\pi_c\left(\mathbf{s}_t, \mathcal{P}\left(\mathbf{s}_t, \epsilon\right)\right) + \mu_c\left(\mathbf{s}_t, \mathcal{P}\left(\mathbf{s}_t, \epsilon\right)\right) \nabla V\left(\mathbf{s}_t, \epsilon\right) = 0.$$

Following Gaspar and Judd (1997), the perturbation technique is based on the computation of a Taylor approximation for the unknown functions $V(\mathbf{s}_t, \epsilon)$ and $\mathcal{P}(\mathbf{s}_t, \epsilon)$ that take into account not only deviations of the state variables from their steady-state values $\hat{\mathbf{s}}_t \equiv (\mathbf{s}_t - \mathbf{s}^{ss})$, but also deviations from the deterministic model as measured by ϵ. In particular, the second-order perturbation, expressed in its tensor form, is given by

$$\tilde{V}\left(\mathbf{s}_t, \epsilon\right) = V^{ss,0} + V_i^{ss,0}\hat{\mathbf{s}}_t^i + V_\epsilon^{ss,0}\epsilon + V_{i\epsilon}^{ss,0}\hat{\mathbf{s}}_t^i\epsilon + \frac{1}{2}V_{ij}^{ss,0}\hat{\mathbf{s}}_t^i\hat{\mathbf{s}}_t^j + \frac{1}{2}V_{\epsilon\epsilon}^{ss,0}\epsilon^2,$$

$$\tilde{\mathcal{P}}\left(\mathbf{s}_t, \epsilon\right) = \mathcal{P}^{ss,0} + \mathcal{P}_i^{ss,0}\hat{\mathbf{s}}_t^i + \mathcal{P}_\epsilon^{ss,0}\epsilon + \mathcal{P}_{i\epsilon}^{ss,0}\hat{\mathbf{s}}_t^i\epsilon + \frac{1}{2}\mathcal{P}_{ij}^{ss,0}\hat{\mathbf{s}}_t^i\hat{\mathbf{s}}_t^j + \frac{1}{2}\mathcal{P}_{\epsilon\epsilon}^{ss,0}\epsilon^2,$$

where $V^{ss,0} \equiv V(\mathbf{s}^{ss}, 0)$, $V_i^{ss,0} \equiv \sum_i \frac{\partial V(\mathbf{s}^{ss},0)}{\partial \mathbf{s}_t^i}$, $V_\epsilon^{ss,0} \equiv \frac{\partial V(\mathbf{s}^{ss},0)}{\partial \epsilon}$, $V_{i\epsilon}^{ss,0} \equiv \sum_i \frac{\partial V(\mathbf{s}^{ss},0)}{\partial \mathbf{s}_t^i \partial \epsilon}$, $V_{ij}^{ss,0} \equiv \sum_i \sum_j \frac{\partial^2 V(\mathbf{s}^{ss},0)}{\partial \mathbf{s}_t^i \partial \mathbf{s}_t^j}$, and $V_{\epsilon\epsilon}^{ss,0} \equiv \frac{\partial^2 V(\mathbf{s}^{ss},0)}{\partial \epsilon^2}$ for $i, j = \{1, \ldots, m\}$ and where $\hat{\mathbf{s}}_t^i$ denotes the ith component of the vector $(\mathbf{s}_t - \mathbf{s}^{ss})$. For the policy function approximation a similar notation is used for each of its n components.

The constant terms in the approximations are given by the deterministic steady state of the model. As shown in Gaspar and Judd (1997) and Judd (1998) the terms associated with the first-order approximation of the policy function, i.e., $\mathcal{P}_i^{ss,0}$ for all $i \in \mathbf{s}$ and every n, correspond to the solution of a Ricatti equation with l roots, where l is the number of equilibrium paths. Once the stable path is chosen, the first-order approximation is completed and the computation of higher-order terms becomes relatively simple since they are defined by the solution of linear systems of equations.[3]

The main difference between perturbation methods for discrete-time and continuous-time models is the existence of certainty equivalence. In discrete-time, the first-order terms associated with the perturbation parameter are always zero regardless of the properties of the economic model, making linearization and first-order perturbation an equivalent procedure [see Judd (1998), Binsbergen et al. (2012), and Caldara et al. (2012)]. However, as discussed in Judd (1996) and in Gaspar and Judd (1997), the approximation of continuous-time stochastic problems will display certainty equivalence if and only if the economic model exhibits the property itself; for example, when the utility function is quadratic and/or the diffusion terms are not only control but state independent. In this case, first-order perturbation and linearization methods are not equivalent. This difference

https://doi.org/10.1017/S1365100516000821 Published online by Cambridge University Press

is particularly relevant for the computation of time-varying risk premia in macro-finance models. While discrete-time models require a third-order perturbation to achieve such time variation, continuous-time models only require a second-order perturbation given that a first-order approximation already delivers a constant premium.

2.3. Projection Methods

Projection-based methods are a widely used technique in applied mathematics and numerical analysis to solve infinite-dimensional functional equations like the HJB equation. It does so by approximating the unknown function by the closest function in the polynomial space. This strategy transforms the original problem into the problem of finding the coefficients of the approximating function.

Formally, let $\mathcal{N}_1(V(\mathbf{s}_t)) = 0$ denote the functional operator defined by the HJB, i.e., it defines a continuous operator that maps all possible value functions into the HJB equation. In particular, this map is given by:

$$\mathcal{N}_1(V(\mathbf{s}_t)) := \max_{\mathbf{c}_t} \left\{ \pi(\mathbf{s}_t, \mathbf{c}_t) - \rho V(\mathbf{s}_t) + \mu(\mathbf{s}_t, \mathbf{c}_t) \nabla V(\mathbf{s}_t) + \frac{1}{2} \text{trace}\left(\Sigma(\mathbf{s}_t) \nabla^2 V(\mathbf{s}_t)\right) \right\} = 0,$$

where $\mathbf{c}_t$ is computed from the first-order conditions of the problem in equation (3).

Let $\mathcal{Q} = \{\phi_k\}_{k=0}^K$ be a given family of univariate polynomials. The first step of any projection method is to assume a parametric approximation for the unknown real-valued function $V(\mathbf{s}_t)$:

$$\tilde{V}(\mathbf{a}, \mathbf{s}_t) = \Phi(\mathbf{s}_t)\mathbf{a}, \quad \mathbf{s}_t \in \mathbf{S} \subset \mathbf{R}_+^m,$$

where $\mathbf{a} = (a_0, \ldots, a_K)$ and $\Phi(\mathbf{s}_t) = \prod_{i=1}^m \phi_{k_i}^i$ is the m-fold tensor product polynomial for all $k_i = 0, 1, \ldots, K$ and all $i = 1, \ldots, m$[4]. Thus, for each $\mathbf{s}_t \in \mathbf{S} \subset \mathbf{R}_+^m$ the maximized HJB equation becomes:

$$0 = \max_{\mathbf{c}_t} \left\{ \pi(\mathbf{s}_t, \mathbf{c}_t) - \rho\Phi(\mathbf{s}_t)\mathbf{a} + \mu(\mathbf{s}_t, \mathbf{c}_t) \nabla\Phi(\mathbf{s}_t)\mathbf{a} + \frac{1}{2} \text{trace}\left(\Sigma(\mathbf{s}_t) \nabla^2 \Phi(\mathbf{s}_t)\mathbf{a}\right) \right\},$$

with first-order conditions:

$$\pi_c(\mathbf{s}_t, \mathbf{c}_t) + \mu_c(\mathbf{s}_t, \mathbf{c}_t) \nabla\Phi(\mathbf{s}_t)\mathbf{a} = 0,$$

for each $c_t \in \mathbf{c}_t$, where $\nabla\Phi(\mathbf{s}_t)$ and $\nabla^2\Phi(\mathbf{s}_t)$ denote the gradient and Hessian matrix of $\Phi(\mathbf{s}_t)$, respectively. Note that the transformed problem is now finite-dimensional. Instead of looking on the function of spaces for $V(\cdot)$, the task

https://doi.org/10.1017/S1365100516000821 Published online by Cambridge University Press

is to compute the $(K+1)$ coefficients $\{a_k\}_{k=0}^{K}$ such that the residual function, $R(\mathbf{a};\mathbf{s}_t) := \mathcal{N}_1(\tilde{V}(\mathbf{a},\mathbf{s}_t))$, is "as close to" zero as possible.

The second part of any projection method is to define a measure of "closeness". Different projection methods imply different conditions on the residual function when evaluated at different grid points. In particular, I consider two types of projections: the least-squares projection method and the collocation method. The former searches for the vector of parameters, $\mathbf{a}^{\text{LS}}$, that minimizes the sum of squared residuals along all the grid points, whereas the latter looks for the vector of parameters, $\mathbf{a}^{\text{COL}}$, that makes the residual function zero at all grid points. The implementation relies on a numerical optimization algorithm to find $\mathbf{a}^{\text{LS}}$ and on a root-finding algorithm to find $\mathbf{a}^{\text{COL}}$. A detailed formulation of the different projections can be found in Judd (1998) and Heer and Maussner (2009).[5]

When the problem at hand is highly non-linear, it is useful to make a simple extension of the method described above. In order to give more flexibility to the approximation and increase the accuracy of the algorithms, it is recommendable to apply the projection technique to more than one functional equation. In particular, it is optimal to approximate not only the HJB equation but also the policy functions resulting from the non-linear first-order conditions, that is:

$$\begin{bmatrix} \mathcal{N}_1\left(V\left(\mathbf{s}_t\right)\right) \\ \mathcal{N}_2\left(\mathcal{P}\left(\mathbf{s_t}\right)\right) \end{bmatrix} = \mathbf{0},$$

where the second set of equations comes from the first-order conditions of the stochastic control problem:

$$\mathcal{N}_2\left(\mathcal{P}\left(\mathbf{s_t}\right)\right) := \pi_c\left(\mathbf{s}_t, \mathcal{P}\left(\mathbf{s_t}\right)\right) + \mu_c\left(\mathbf{s}_t, \mathcal{P}\left(\mathbf{s_t}\right)\right) \nabla V\left(\mathbf{s}_t\right) = 0.$$

I now define two different parametric approximations:

$$\tilde{V}\left(\mathbf{a},\mathbf{s}_t\right) = \Phi_a\left(\mathbf{s}_t\right)\mathbf{a} \quad \text{and} \quad \tilde{\mathcal{P}}\left(\mathbf{b},\mathbf{s}_t\right) = \Phi_b\left(\mathbf{s}_t\right)\mathbf{b}, \quad \forall \mathbf{s}_t \in \mathbf{S} \subset \mathbf{R}_+^m,$$

which allow for more flexibility in the approximation through different basis functions and basis points for each of the functional equations. Under this extension, the problem becomes that of finding two different set of parameters $\mathbf{a}$ and $\mathbf{b}$ such that the residual function $R(\mathbf{a},\mathbf{b};\mathbf{s}_t) := [\mathcal{N}_1(\tilde{V}(\mathbf{a},\mathbf{s}_t)), \mathcal{N}_2(\tilde{\mathcal{P}}(\mathbf{b},\mathbf{s}_t))]^\top$ is "as close to" zero as possible.

Regarding the selection of $\mathcal{Q}$, I choose the set of orthogonal polynomials generated by the Chebyshev function. The grid or nodal points of the state vector used in the approximation correspond to the zeros of the Chebyshev polynomials. The combination of Chebyshev basis and nodes yields an extremely well-behaved projection equation that can be solved accurately and efficiently even for high degrees of approximation [Judd (1998)]. For this choice, the state variables in $\mathbf{S} \subset \mathbf{R}_+^m$ must be transformed from their original domain since the Chebyshev polynomials are only defined in $[-1, 1]$. This is achieved by using the map

https://doi.org/10.1017/S1365100516000821 Published online by Cambridge University Press

$\Gamma(s_t^j) = (2s_t^j - \underline{s}^j - \overline{s}^j)/(\overline{s}^j - \underline{s}^j)$, where $s_t^j \in [\underline{s}^j, \overline{s}^j]$ and $\underline{s}^j$, $\overline{s}^j$ are the predefined bounds of the jth state variable.

3. BENCHMARK MODEL

I consider, as a test case, a modified version of the Real Business Cycle (RBC) model described in Aruoba et al. (2006) where time is continuous, the capital stock is subject to random shocks, and shocks to total factor productivity (TFP) are heteroscedastic. The one-good in this economy is produced according to a constant return to scale technology:

$$Y_t = A_t K_t^{\alpha} L_t^{1-\alpha}, \quad \alpha \in (0, 1), \tag{5}$$

where A_t denotes the stationary TFP, K_t the aggregate capital stock, and L_t the fraction of hours worked. I assume that the TFP is driven by a Cox–Ingersoll–Ross (CIR) mean reverting stochastic process of the form:

$$\mathrm{d}A_t = \kappa\,(\omega - A_t)\,\mathrm{d}t + \eta\sqrt{A_t}\mathrm{d}B_{A,t}, \qquad \kappa, \omega > 0 \text{ and } A_0 > 0 \text{ given}, \tag{6}$$

where $B_{A,t}$ is a standard Brownian motion and $\eta > 0$ denotes the volatility of the TFP. This process ensures that the random variable A_t only takes positive values.

On the other hand, aggregate capital, K_t, is accumulated according to

$$\mathrm{d}K_t = (I_t - \delta K_t)\,\mathrm{d}t + \sigma K_t \mathrm{d}B_{K,t}, \quad K_0 > 0 \text{ given}, \tag{7}$$

where I_t is the gross rate of investment, $\delta > 0$ is the depreciation rate, and $B_{K,t}$ an exogenous aggregate Brownian shock with volatility $\sigma > 0$. These shocks can be interpreted as exogenous variation in the marginal efficiency of investment and/or in the future productivity of the capital stock as justified in Furlanetto and Seneca (2014) and Brunnermeier and Sannikov (2014). In particular, these shocks represent changes in the firm's expected future cash flows that could undercapitalize the firm, or alter its balance sheet. Alternative interpretations of shocks to capital accumulation can be found in Wälde (2011) and Gourio (2012).

The representative firm producing the one-good in the economy is owned by households and assumed to operate in competitive markets. The optimal demands for capital and labor are:

$$r_t = \alpha A_t K_t^{\alpha-1} L_t^{1-\alpha} \quad \text{and} \quad w_t = (1-\alpha)\, A_t K_t^{\alpha} L_t^{-\alpha}, \tag{8}$$

where r_t is the rental rate of capital and w_t is the real wage rate.

Following Turnovsky and Smith (2006) and Posch (2011), the representative household maximizes the expected discounted life-time utility derived from

https://doi.org/10.1017/S1365100516000821 Published online by Cambridge University Press

consumption, C_t, and leisure, $(1 - L_t)$:

$$\max_{\{C_t, L_t\}_{t=0}^{\infty}} \mathbf{E}_0 \int_0^{\infty} e^{-\rho t} \frac{\left(C_t \left(1 - L_t\right)^{\psi}\right)^{1-\gamma}}{1-\gamma} \mathrm{d}t, \quad \psi \geq 0, \gamma > 0,$$

subject to the intertemporal budget constraint

$$\mathrm{d}K_t = \left(\left(r_t - \delta\right) K_t + w_t L_t - C_t\right) \mathrm{d}t + \sigma K_t \mathrm{d}B_{K,t}, \tag{9}$$

where $\rho > 0$ is the rate of time preference, ψ measures preference for leisure, and γ denotes the inverse of the intertemporal elasticity of substitution (IES). To ensure concavity of the utility function the consumption–leisure measure of relative risk aversion has to be greater or equal to zero, i.e., $\gamma - (1 - \gamma)\psi \geq 0$ [Swanson (2012)].

Under competitive markets the equilibrium allocations in a decentralized economy coincide with those of a social planner: A benevolent planner maximizes the utility of the representative household subject to the production function [equation (5)], the evolution of the TFP [equation (6)], the evolution of the capital stock [equation (7)], the market clearing condition $Y_t = C_t + I_t$ and some initial values $K_0 > 0$ and $A_0 > 0$. The first-order conditions for any interior solution are:

$$\frac{\left(C_t \left(1 - L_t\right)^{\psi}\right)^{1-\gamma}}{C_t} = V_K \left(K_t, A_t\right), \tag{10}$$

$$\psi \frac{\left(C_t \left(1 - L_t\right)^{\psi}\right)^{1-\gamma}}{\left(1 - L_t\right)} = (1 - \alpha) A_t K_t^{\alpha} L_t^{-\alpha} V_K \left(K_t, A_t\right), \tag{11}$$

making optimal consumption and the optimal fraction of hours worked implicit functions of the state variables, i.e., $C_t = C\left(K_t, A_t\right)$ and $L_t = L\left(K_t, A_t\right)$. The solution to the planner's problem is fully characterized by the maximized (concentrated) HJB equation:

$$\begin{aligned} \rho V \left(K_t, A_t\right) = & \frac{\left(C \left(K_t, A_t\right) \left(1 - L \left(K_t, A_t\right)\right)^{\psi}\right)^{1-\gamma}}{1-\gamma} \\ & + \left(A_t K_t^{\alpha} L \left(K_t, A_t\right)^{1-\alpha} - \delta K_t - C \left(K_t, A_t\right)\right) V_K \left(K_t, A_t\right) \\ & + \kappa \left(\omega - A_t\right) V_A \left(K_t, A_t\right) + \frac{1}{2} \sigma^2 K_t^2 V_{KK} \left(K_t, A_t\right) + \frac{1}{2} \eta^2 A_t V_{AA} \left(K_t, A_t\right), \end{aligned} \tag{12}$$

for any $t \in [0, \infty)$ and where $V(K_t, A_t)$ is the value function and denotes the value at instant t of the planner's expected utility along the optimal program. Equation (12) defines a functional equation in the unknown value and policy functions. Solving for the equilibrium of this economy amounts to find in the

https://doi.org/10.1017/S1365100516000821 Published online by Cambridge University Press

space of functions for $V(K_t, A_t)$, $C(K_t, A_t)$, and $L(K_t, A_t)$ such that given a random path for the exogenous process, $\{A_t\}_{t=0}^{\infty}$, and an initial condition $K_0 > 0$:

1. the planner solves his problem, i.e., equation (12) is satisfied at every instant of time,
2. the accumulation constraints (6) and (7) are satisfied at every instant of time, and
3. the goods market clears, $Y_t = C_t + I_t$.

In general, the planner's problem does not admit a closed-form solution. However, under some parametric restrictions it is possible to derive analytical expressions for the value and policy functions. The parameterizations under which it is possible to derive a closed-form solution provide a benchmark to assess the accuracy of the numerical approximations.

PROPOSITION 3.1 (*Constant savings function). Suppose that total factor productivity is constant, i.e.,* $A_t = \bar{A}$. Let $\psi > 0$, $\gamma \geq 1$ and $\rho = \bar{\rho}$ *with*

$$\bar{\rho} = -(1-\alpha\gamma)\left(\delta + \frac{1}{2}\alpha\gamma\sigma^2\right) > 0,$$

then, the value function is given by

$$V(K_t, \bar{A}) = \Gamma \frac{K_t^{1-\alpha\gamma}}{1-\alpha\gamma}, \tag{13}$$

where the constant Γ *is given by*

$$\Gamma = \left(-\frac{(1-s)^{(1-\gamma)}\,\bar{A}^{(1-\gamma)}L^{(1-\alpha)(1-\gamma)}(1-L)^{\psi(1-\gamma)}}{(1-\gamma)\,\bar{A}L^{(1-\alpha)} - (1-\gamma)\,(1-s)\bar{A}L^{(1-\alpha)}}\right),$$

and

$$1 - s \equiv \frac{(1-\alpha)\,(1-L)}{\psi L}$$

denotes the constant propensity to consume out of income. Then, the optimal consumption will be a constant fraction of income:

$$C(K_t, \bar{A}) = (1-s)\bar{A}K_t^{\alpha}L^{1-\alpha}, \tag{14}$$

and the optimal fraction of hours supplied will be constant:

$$L(K_t, \bar{A}) = \frac{\gamma(1-\alpha)}{\gamma(1-\alpha) - \psi(1-\gamma)} \in [0, 1]. \tag{15}$$

Proof. See Posch (2011) ■

Using equations (6)–(8), (10), and (11) together with the first-order derivatives of equation (12) with respect to the state variables, it is possible to derive the deterministic steady state of the economy. This is given by the quantities: $r^{ss} = \rho + \delta$, $A^{ss} = \omega$, $L^{ss} = {}^{(1-\alpha)}/_{(1+\psi-\alpha-\frac{\alpha\psi\delta}{\rho+\delta})}$, $K^{ss} = (\alpha A^{ss}/(\rho+\delta))^{\frac{1}{1-\alpha}}L^{ss}$, $w^{ss} = (1-\alpha)A^{ss}(K^{ss})^{\alpha}(L^{ss})^{-\alpha}$, $C^{ss} = (r^{ss}-\delta)K^{ss} + w^{ss}L^{ss}$, and $V^{ss} = {}^{(C^{ss}(1-L^{ss})^{\psi})^{1-\gamma}}/_{\rho(1-\gamma)}$,

https://doi.org/10.1017/S1365100516000821 Published online by Cambridge University Press

which will be used for the implementation of the perturbation method and the LQ approximation.

The model just outlined has an equivalent representation with investment and leisure as control variables. Under this alternative setup the drift of the stochastic differential equation describing the capital stock is linear in the control and state variables. This formulation will be used later to compute an alternative LQ approximation of the policy functions with correct coefficients as mentioned in Section 2.1. This representation can be found in Appendix A.1.

4. NUMERICAL RESULTS

4.1. Calibration

To evaluate the performance of the different numerical methods I carry out two types of exercises. First, I use the analytical solution in Proposition 3.1 to assess their accuracy by comparing deviations of the numerical approximations from the true solution. Later, I use the model without parametric restrictions and evaluate their relative performance using a different set of accuracy measures.

The parameter values used in both exercises are taken from Aruoba et al. (2006) and match some salient features of the US economy. They are reported in the last column of Table 1. The rate of time preference is set to $\rho = 0.0105$ to match a 4% annual interest rate; the risk aversion parameter γ is fixed to 2, a value widely used in the literature; the share of labor in aggregate output and the depreciation rate are set to $\alpha = 0.4$ and $\delta = 0.0196$, respectively, whereas the leisure preference parameter is fixed to $\psi = 1.8011$ to match a labor supply of 31% in the steady state. Regarding the stochastic components of the model, the volatility of the capital stock accumulation is set equal to zero to match the calibration used in Aruoba et al. (2006), whereas κ, ω, and η are chosen to match the properties of the Solow residual in the US economy. In particular, $\eta = 0.007$ and $\kappa = 0.05$ closely match the statistical properties of the Solow residual derived from equation (5) under the assumption that changes in the quarterly stock of capital are approximately zero. This choice of parameters implies a model's output volatility of Std[log (Y_t)] = 1.09% per quarter, close to that observed in the post-war period, Std[log (GDP)] = 0.96%.

However, the first exercise uses the modified parameterization reported in the first column of Table 1, which allows me to use the closed-form solution in Proposition 3.1. The risk aversion parameter is then set to 3.85 to obtain a "knife-edge" value for the rate of time preference, $\bar{\rho}$, close to 0.0105; the TFP is fixed to $A_t = \bar{A} = 1$ for all t; and to allow for some randomness I set the standard deviation of the shocks to the capital stock, σ, to be 0.001.

In Section 4.3, the second exercise is repeated using alternative calibrations in order to check the robustness of the solution methods to different degrees of nonlinearities of the model arising from the risk aversion parameter and the volatility of the disturbances. Table 2 summarizes the alternative scenarios.

https://doi.org/10.1017/S1365100516000821 Published online by Cambridge University Press

TABLE 1. Benchmark calibration

Parameter	Analytical sol.	No analytical sol.
ρ	$\bar{\rho}$	0.0105
ψ	1.8011	1.8011
γ	3.85	2.00
α	0.4	0.4
δ	0.0196	0.0196
σ	0.001	0.000
κ	N.A.	0.05
ω	N.A.	1.00
η	N.A.	0.007
$\bar{A}$	1.00	N.A

In the model, time is measured in quarters and parameter values should be interpreted accordingly. The aggregate capital stock in the economy evolves according to

$$dK_t = \left(A_t K_t^{\alpha} L_t^{1-\alpha} - \delta K_t - C_t\right) dt + \sigma K_t dB_{K,t},$$

where $B_{K,t}$ is a standard Brownian motion. The dynamics of total factor productivity is given by

$$dA_t = \kappa\left(\omega - A_t\right) dt + \eta\sqrt{A_t} dB_{A,t},$$

where $B_{A,t}$ is a standard Brownian motion independent of $B_{K,t}$. The representative agent has standard preferences defined by $V_t = \mathbf{E}_t\left[\int_t^{\infty} e^{-\rho t} u\left(C_s, L_s\right) ds\right]$, where

$$u\left(C_t, L_t\right) = \frac{\left(C_t\left(1 - L_t\right)^{\psi}\right)^{1-\gamma}}{1-\gamma}.$$

TABLE 2. Sensitivity analysis

	$\eta = 0.007$		$\eta = 0.035$	
Case	$\sigma = 0.000$	$\sigma = 0.001$	$\sigma = 0.000$	$\sigma = 0.001$
$\gamma = 0.65$	M1	M3	M6	M8
$\gamma = 2$	Benchmark	M4	M7	M9
$\gamma = 10$	M2	M5	Extreme I	Extreme II

The value $\gamma = 0.65$ was chosen in such a way that the concavity condition for the utility function was fulfilled given the calibrated value of ψ.

4.2. Value Function, Policy Functions, and HJB Equation Residuals

Figure 1 plots the approximated value and policy functions and their corresponding true values under Proposition 3.1. From the analytical solution it is clear that the value function exhibits a very steep slope for low values of the capital stock. Therefore, it seems relevant to include values of the capital stock that are away from its deterministic steady state in order to compare the performance of the approximation methods around regions where the value function is highly non-

https://doi.org/10.1017/S1365100516000821 Published online by Cambridge University Press

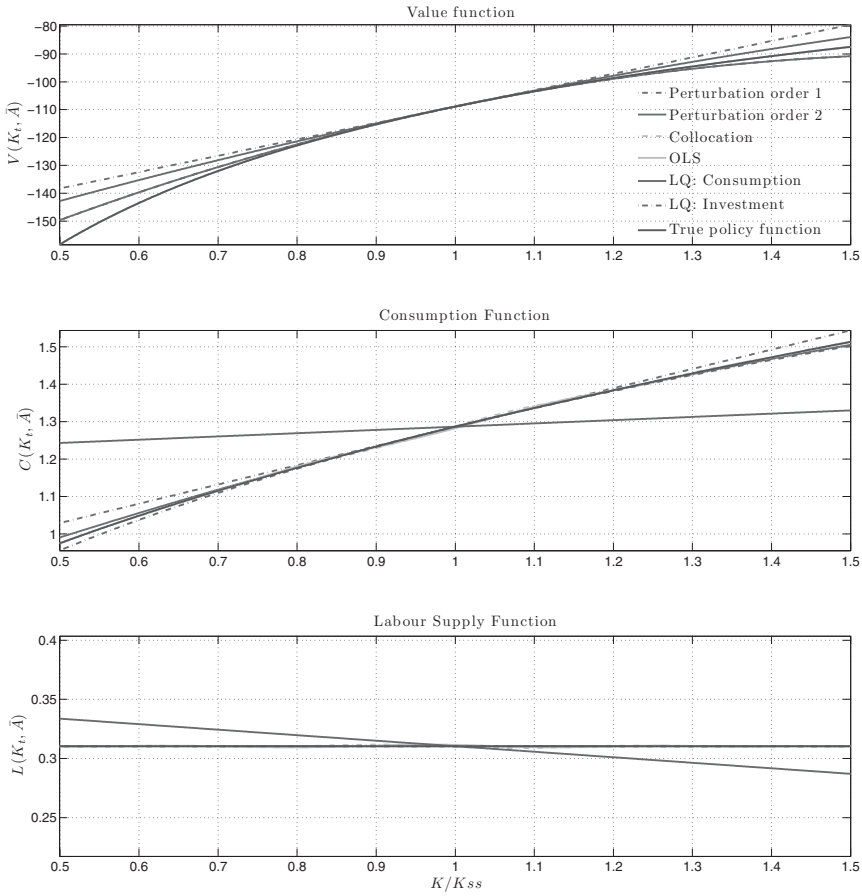

FIGURE 1. Approximated vs. true value and policy functions. The graph plots the value function and the policy functions for consumption and labor supply along the interval $[0.5K^{ss}, 1.5K^{ss}]$ using different approximation methods as well as the closed form representation available under Proposition 3.1.

linear. The approximations are computed along the interval $[0.5K^{ss}, 1.5K^{ss}]$. For projection methods, I first compute a 17th degree Chebyshev approximation using the true function values as a starting point. Given the width of the state-space, a fewer number of nodes result in non-accurate and non-smooth policy functions. Once the coefficients of the approximated solution are found, I use linear interpolation on a set of $n_K = 1000$ equally spaced points to evaluate the accuracy of the method. The same number of equally spaced points in the state-space are used to evaluate the local approximation methods.[6]

As expected from theory, global approximations (projection methods) outperform local approximations (perturbation and LQ approximations) for levels of the

https://doi.org/10.1017/S1365100516000821 Published online by Cambridge University Press

capital stock away from its steady state. However, note the improvement obtained by moving from a first to a second-order perturbation, in particular, the correction of about 100% in the curvature of the value function at the lower bound of the grid. Hence, provided that such an approximation remains within the radius of convergence as we increase the order of perturbation, this result encourages the computation of higher-order perturbations which, as will be shown later, come at no significant extra computing cost.

Regarding the accuracy of the LQ approximation, two points are worth to mention. First, when the "naive" LQ approximation is used, the slopes of the policy functions are miscalculated as discussed in Section 2.1. This can be easily identified in the middle panel of Figure 1 under the label *LQ:consumption.* However, if the equivalent representation described in Appendix A.1 is used, the slopes of the approximations are correctly computed as shown by *LQ:investment*. Since the restrictions of the alternative optimization problem are linear, no information is lost in the approximation step of the objective function. Second, the effect of linear vs. linearized budget constraints affects the approximation of the value function in a less considerable way.

To complement the previous findings, I compute the following measures introduced in Collard and Juillard (2001) to evaluate the quality of the approximations:

$$E_1^l = 100 \times \frac{1}{n_K} \sum_{i=1}^{n_K} \left| \frac{f\left(K_i, A^{ss}\right) - \hat{f}^l\left(K_i, A^{ss}\right)}{f\left(K_i, A^{ss}\right)} \right|,$$

and

$$E_\infty^l = 100 \times \max_i \left\{ \left| \frac{f\left(K_i, A^{ss}\right) - \hat{f}^l\left(K_i, A^{ss}\right)}{f\left(K_i, A^{ss}\right)} \right| \right\},$$

where $f(K_i, A^{ss})$ denotes the true solution of either the value or the policy functions evaluated at grid point i, $\hat{f}^l(K_i, A^{ss})$ the approximation obtained by method l evaluated at grid point i, and n_K the number of grid points in the state-space. The statistic E_1^l measures the average relative error of using the approximation instead the true solution, whereas E_∞^l measures the maximum relative error. Sometimes, the latter is preferred since it bounds the error made by using the approximation instead of the true function [Aruoba et al. (2006)]. The results are shown in Table 3.

Overall, the results suggest the use of projection methods over the alternatives for the solution of continuous-time DSGE models: a maximum error of 0.16% for the case of the value function when using collocations. However, as it will be shown later, a greater level of accuracy requires more computing time relative to perturbation or LQ methods, which might relegate it from an econometric perspective where the solution of the model is needed at each iteration of the estimation procedure, e.g., maximum likelihood. On the other hand, one alternative to improve the accuracy of perturbation for any given degree of approximation is to use rational functions. This parametric method, known as Padé approximations,

https://doi.org/10.1017/S1365100516000821 Published online by Cambridge University Press

TABLE 3. Accuracy check for benchmark model under Proposition 3.1 (%)

	Value function		Consumption		Labor supply	
Method	E_1	E_∞	E_1	E_∞	E_1	E_∞
Perturbation 1	11.2008	57.1436	6.8988	60.7601	0.0000	0.0001
Perturbation 2	6.6285	47.4301	3.1341	36.3450	0.0000	0.0000
Collocation	0.0275	0.1592	0.0948	0.4635	0.1201	0.5224
Least squares	0.0229	0.0904	0.0962	0.3863	0.1186	0.4430
LQ (cons.)	9.1221	53.3116	24.2086	135.8970	5.6952	13.5280
LQ (inv.)	6.6287	47.4303	2.4204	21.3193	0.0003	0.0004

The table reports the average relative error, E_1, and the maximum relative error E_∞ between the approximated and true policy functions using each of the different approximation methods in percentage terms. Results are reported for the value function and the policy functions for consumption and labor supply.

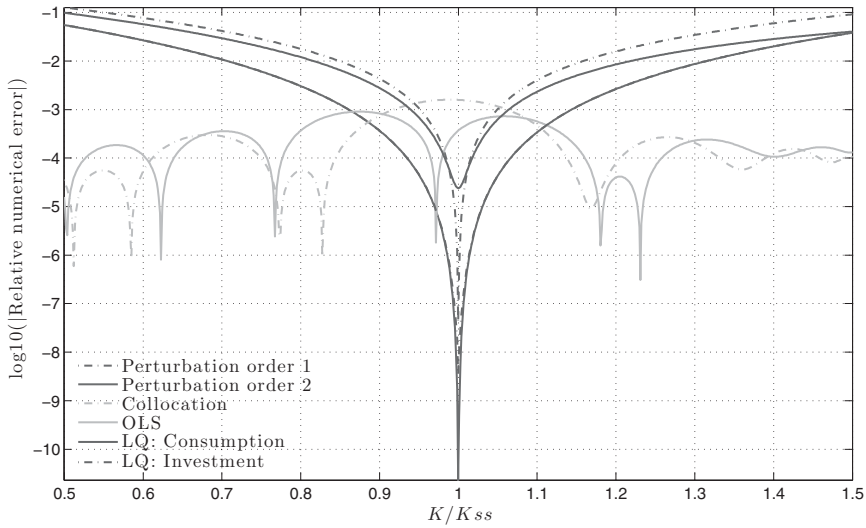

FIGURE 2. Numerical error for benchmark model under Proposition 3.1. The graph plots the log10 magnitude of the relative numerical error made by using the approximated value function along the interval $[0.5K^{ss}, 1.5K^{ss}]$. The error is relative to the true value function.

has been proven to perform better away from the steady state. Judd and Guu (1993) discuss its application in the context of a one state–one control variable continuous-time stochastic growth model.[7]

Figure 2 plots the log10 magnitude of the relative numerical error obtained from the approximation of the value function along all the state-space. A value of -6 indicates that for every million of units of welfare, the agent makes an error of 1 unit by using the approximation instead of the true function. The plot depicts the global nature of projection methods as well as the local nature of perturbation and

https://doi.org/10.1017/S1365100516000821 Published online by Cambridge University Press

LQ methods where the approximation deteriorates as the capital stock moves away from the steady state. However, note how the use of a second-order perturbation or a LQ approximation with linear constraints reduces this error.

Next, I consider the general case where no closed-form solution is available. The state-space in this scenario is given by $\mathbf{R}^2_+$. The approximations are computed over $[0.5K^{ss}, 1.5K^{ss}] \times [\underline{A}, \overline{A}]$ where the grid along the TFP lattice is designed following Heer and Maussner (2009): I set $(\overline{A} - \underline{A})$ equal to a multiple of $\sigma_A = \sqrt{\omega(\eta^2/2\kappa)}$, which corresponds to the limiting standard deviation of equation (6).[8] In particular, the grid for the TFP is defined as $[A^{ss} - 5\sigma_A, A^{ss} + 5\sigma_A]$ which for the AR(1) discrete-time representation of the Ornstein–Uhlenbeck process has been shown to be a reasonably good approximation.

Projection methods use nine Chebyshev basis functions, and their initial values are set according to the following rule-of-thumb: first obtain a local approximation by means of a first-order perturbation; and then use this as an initial guess for the least-squares approximation. Once a reasonable approximation has been found (usually before 100,000 iterations using a *trust-region-dogleg* algorithm), use it as an initial guess for the collocation method. When the latter converges, use it as a starting value for the least-squares algorithm again to check for robustness. I use the least-squares residual function first since it is less demanding in terms of the projection criterion.

Figure 3 plots the value and policy functions for each of the numerical methods using 301 grid points in each lattice and fixing the TFP at its steady-state value. Plots for different values of the TFP can be easily derived and are available upon request. A similar pattern to that described previously is obtained. All the approximations are almost indistinguishable around the steady-state value of the capital stock. However, some differences are found when moving away from that point. In particular, *LQ:consumption* and perturbation of order one tend to diverge outside the steady state from the approximations obtained by *LQ:investment*, second-order perturbation, and projection methods.

The statistics E_1 and E_∞ defined previously cannot be used to evaluate the performance of the different approximation methods since no closed-form solution is available.[9] Therefore, I follow Judd and Guu (1993) and compute the unit free vector of HJB equation residuals for each of the procedures. A similar measure, usually called Euler equation errors, is used in discrete-time analysis of DSGE models.[10] The idea is to check how much $\mathcal{N}_1(\hat{V}(K_i, A_j))$ for $i = 1, \ldots, n_K$, $j = 1, \ldots, n_A$, as a fraction of the discounted steady-state value function, differs from the zero function.[11] I define the HJB equation residuals as:

$$R^l_{\text{HJB}}\left(K_i, A_j\right) \equiv \left(\frac{\mathcal{N}_1\left(\hat{V}^l\left(K_i, A_j\right)\right)}{\rho \hat{V}^l\left(K^{ss}, A^{ss}\right)}\right),$$

for all i, j in the state-space and approximation method l.[12] This measure can be interpreted as the relative optimization error incurred by the use of the approximated value and policy functions. It is an optimization error since the residuals

https://doi.org/10.1017/S1365100516000821 Published online by Cambridge University Press

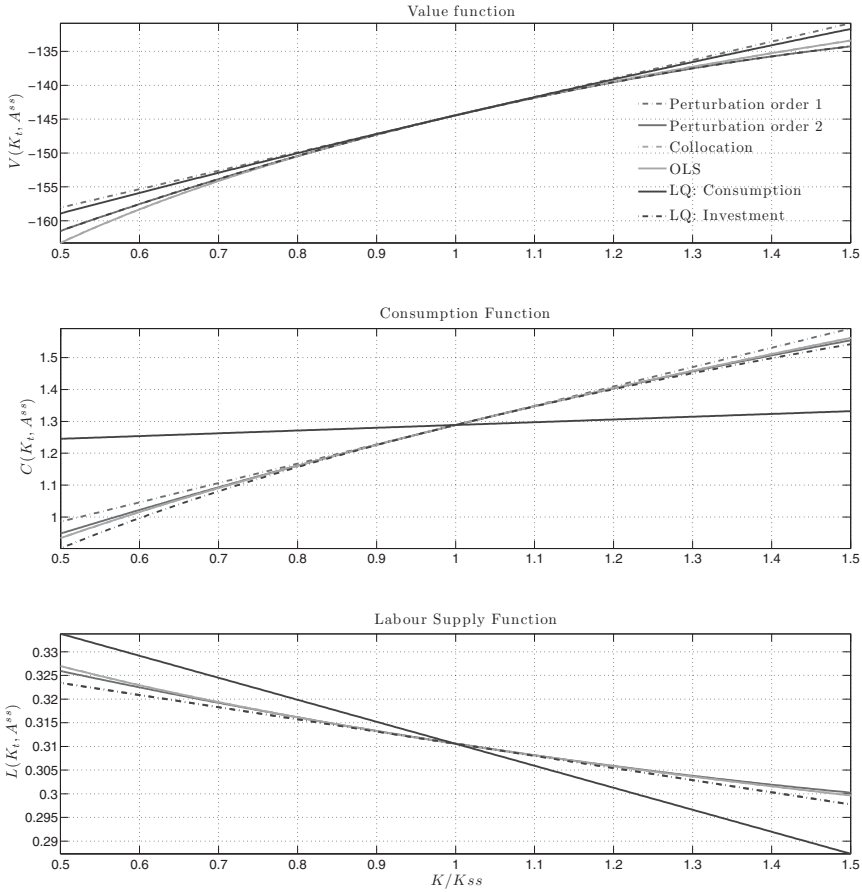

FIGURE 3. Approximated value and policy functions for benchmark calibration. The graph plots the value function and the policy functions for consumption and labor supply along the interval $[0.5K^{ss}, 1.5K^{ss}]$ and $A_t = A^{ss}$ using different approximation methods.

are computed from the maximized HJB equation. The results are summarized in Table 4 where I have computed the statistics:

$$\tilde{E}_1^l = \frac{1}{n_A n_K} \sum_{j=1}^{n_A} \sum_{i=1}^{n_K} R_{\text{HJB}}^l \left(K_i, A_j\right) \text{ and } \tilde{E}_\infty^l = \max_{i,j} \left\{ R_{\text{HJB}}^l \left(K_i, A_j\right) \right\},$$

where $\tilde{E}_1^l$ is the average HJB equation residual and $\tilde{E}_\infty^l$ is the maximum HJB equation residual. As before, the maximum HJB equation residual bounds the error made by using a particular approximation method. Once again global methods outperform local methods. Furthermore, the differences between first- and second-order perturbation indicate that the increase in the order of approximation reduces

https://doi.org/10.1017/S1365100516000821 Published online by Cambridge University Press

TABLE 4. HJB residuals for benchmark calibration

Method	$\tilde{E}_1$	$\tilde{E}_\infty$
Perturbation 1	−1.6243	−0.5889
Perturbation 2	−2.3272	−0.8374
Collocation	−5.4546	−4.8822
Least Squares	−5.3024	−4.5718
LQ (cons.)	−0.8691	−0.1122
LQ (inv.)	−0.6340	−0.1147

The table reports the average HJB residual, $\tilde{E}_1$, and the maximum HJB residual, $\tilde{E}_\infty$, for each of approximation methods when applied to the approximation of the value function.

the numerical error in almost 100%. A similar conclusion is obtained by looking at both types of LQ approximations.

Figure 4 plots a transversal cut of the HJB equation residuals for $A_t = A^{ss}$. Figure A.1 in Appendix A.2 presents the HJB equation residuals on both dimensions of the state-space for each of the numerical procedures. The superiority of global methods relative to perturbation methods in both dimensions of the state-space is clear from the results.

4.3. Robusteness Check

Table 5 reports the maximum HJB equation residuals under the alternative calibrations in Table 2. In particular, I analyze the effects of different values of the risk aversion parameter and of increased volatility of shocks to productivity and capital stock. These alternative scenarios can be used to assess the performance of each of the approximation methods for different degrees of non-linearities in the model. As an example, consider the scenario M7 in Table 2. By increasing the TFP volatility from 0.007 to 0.035, while keeping the remaining parameters fixed at the benchmark calibration, I evaluate the accuracy of the different methods to approximate the solution of a model economy with a quarterly output volatility of approximately 3.89%, that is, 280 basis points higher than in the benchmark economy. The value and policy functions as well as the transversal cuts of the residuals are not plotted due to space considerations but are available upon request.

In terms of the relative performance of the numerical methods, the results are robust to changes in the degree of non-linearities. Nevertheless, global methods require additional computing time to converge relative to the benchmark case, especially when the coefficient of risk aversion is high. In other words, changes in the concavity of the utility function, and hence, in the concavity of the value function reduce the computational efficiency of projection methods. Furthermore, this effect dominates when compared to the additional computing time induced by changes in the variance of the shocks. Despite this result, global methods exhibit a superior level of accuracy relative to perturbations and LQ approximations. The performance of the local methods deeply deteriorates for high levels of the

https://doi.org/10.1017/S1365100516000821 Published online by Cambridge University Press

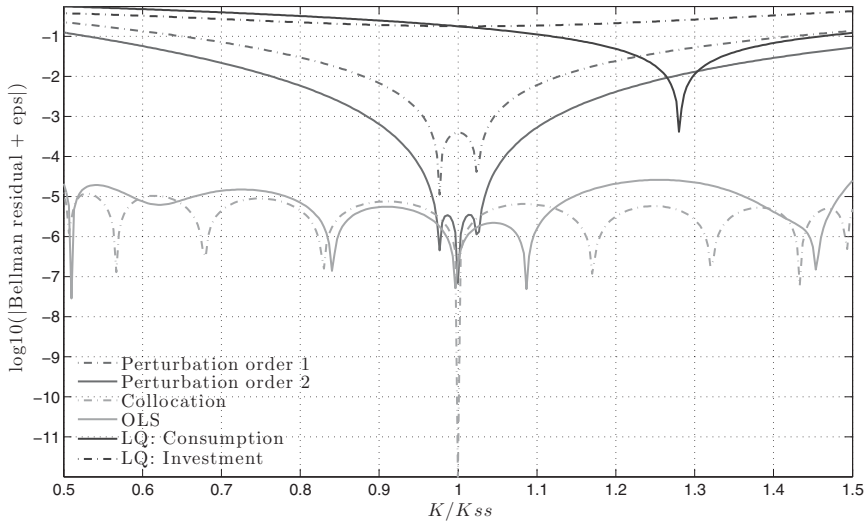

FIGURE 4. HJB residuals for benchmark calibration. The graph plots the log10 magnitude of the HJB residual along the interval $[0.5K^{ss}, 1.5K^{ss}]$ for the different approximation methods.

TABLE 5. Maximum HJB residuals for alternative calibrations

	Pert. 1	Pert. 2	Coll.	LS	LQ (con.)	LQ (inv.)
M1	−0.7104	−1.0813	−2.9793	−2.9793	−0.4211	−0.3793
M2	1.2829	1.2766	−4.4311	−3.7181	1.5801	1.6142
M3	−0.7104	−1.0813	−2.9793	−2.9801	−0.4211	−0.3793
M4	−0.5890	−0.8375	−4.8822	−4.8511	−0.1122	−0.1146
M5	1.2830	1.2766	−4.4313	−4.2401	1.5801	1.6142
M6	−0.5497	−0.7261	−2.4306	−2.4306	−0.0643	0.0441
M7	−0.3938	−0.7039	−3.1427	−3.1254	0.2949	0.4192
M8	−0.5536	−0.7252	−2.4306	−2.4305	−0.0643	0.1070
M9	−0.3984	−0.7039	−3.1456	−3.1476	0.2949	0.4192
Extreme 1	2.8473	2.5840	−2.3470	−2.3740	2.0828	2.2600
Extreme 2	2.8474	2.5841	−2.3742	−2.3742	2.0828	2.2600

The table reports the maximum HJB residual $\tilde{E}_\infty$ for each of approximation methods when applied to the approximation of the value function under the different scenarios of Table 2.

risk aversion parameter as can be seen from HJB equation residuals crossing the zero line under the extreme calibrations and scenarios M2 and M5.[13] Similar conclusions are obtained with the average HJB residuals, $\tilde{E}_1$.

To reduce the impact of non-linearities on the implementation of projection methods the rule-of-thumb suggested in Section 4.2 is complemented in the following recursive manner: Approximate the unknown functions on a narrow grid

https://doi.org/10.1017/S1365100516000821 Published online by Cambridge University Press

for the capital stock, e.g., between $[0.95K^{ss}, 1.05K^{ss}]$, using as an initial guess the solution from perturbation. Once a solution has been found, increase the size of this lattice by a small amount, e.g., $\pm 0.05K^{ss}$, while keeping fixed the number of nodes in both dimensions and using as an initial value the previous solution. Continue in this way until the solution for the desired grid has been found.

Although the accuracy of the different methods is similar to that reported for discrete-time models, two main differences of economic importance emerge when comparing my results to those reported in Aruoba et al. (2006).

First, high levels of risk aversion and extreme values of the volatility of shocks yield levels of consumption and labor supply in the continuous-time setup that differ substantially across approximation methods. On average, labor supply and aggregate consumption are 51% higher and 23% lower respectively when using perturbation and/or LQ methods relative to the levels obtained by projection methods. Although Aruoba et al. (2006) argue that this difference could be explained by the certainty equivalence property that holds for discrete-time models, the fact that first-order perturbation applied to continuous-time models does not exhibit such a property invalidates their argument.

Second, Aruoba et al. (2006) conclude that for levels of $\gamma > 40$, highly risk-averse agents will work hard whenever the capital stock is high in order to accumulate even more capital to insure themselves against unforeseen bad times. In that case, the slope of the labor supply function is shown to switch from negative to positive. However, I find that for the model of Section 3, a value of $\gamma = 10$ already exhibits such a precautionary behavior.

The question of what explains the different levels of the aggregate variables and what is the correct threshold for γ that shifts the slope of the labor supply function remains unanswered and should be addressed in future research.

4.4. A Note on Implementation and Computing Time

I conclude this section with some remarks on the implementation and computing time, although as argued in Aruoba et al. (2006) the running time for each of the algorithms is of minor relevance when compared with the programming and debugging time used in coding. Regarding the implementation, global methods and the LQ approximation are implemented in Matlab® 7.11.0. For projection methods, I rely on the CompEcon Toolbox developed by Miranda and Fackler (2002) to compute the Chebyshev polynomials and the Chebyshev nodes. On the other hand, perturbation methods are implemented in Mathematica® 7.0. The main reason for using a different software for the latter is the inability of the Symbolic Toolbox of Matlab® to compute and evaluate derivatives of implicit functions with respect to the state variables. All the computations are performed in a 2.53 GHz Intel® Core™2 Duo running Windows 7.

In terms of computing time, perturbation methods are the fastest with a first-order approximation taking about 0.049 seconds to deliver the model's solution under the benchmark calibration. The second-order perturbation takes 0.577 sec-

https://doi.org/10.1017/S1365100516000821 Published online by Cambridge University Press

onds. Although using the same local information to compute the approximation, LQ methods require between 0.651 and 2.167 seconds depending on whether the budget constraint is linear or not. Finally, their dependence on an appropriate initial guess makes projection methods the slower among the techniques studied in this article.[14] The collocation method uses 2.976 seconds to approximate the unknown functions, whereas the least-squares method requires 965 seconds. However, it is important to keep in mind that, conditional on an good initial guess, global methods produce approximations that are closer to the true policy functions.

Although not being directly comparable, the previous computing times provide initial and non-formal evidence indicating that continuous-time DSGE models can be solved faster than their discrete-time counterpart. The computing times for the discrete-time version of the benchmark model studied in this paper are reported in Aruoba et al. (2006), and for the case of perturbation and projection methods the authors report much higher running times. A formal assessment of this conclusion should be addressed in future research.

5. CONCLUDING REMARKS

This article describes and compares different numerical methods to approximate the solution of continuous-time DSGE models in the spirit of Taylor and Uhlig (1990), Aruoba et al. (2006), and Caldara et al. (2012). A continuous-time version of the stochastic neoclassical growth model with endogenous labor studied in Aruoba et al. (2006) is used as a test case. Under plausible parameterizations, this version of the model admits a closed-form solution that can be used to check the accuracy of the different solution methods by measuring how far the approximations are from the true solution. When the model is left unrestricted, alternative measures based on the HJB equation residuals are used to evaluate the performance of the approximations. In particular, I compare the results obtained from using (i) LQ approximations; (ii) first and second-order perturbation; and (iii) projection methods.

Similarly to the discrete-time case, I find projection methods to be more accurate and robust than perturbations for a wide range of values of the state-space centered around the deterministic steady state. Their accuracy extends to different degrees of non-linearities. In particular, I study the effect of different values of the risk aversion parameter and higher values of the volatility of the shocks that hit the economy. This becomes a relevant issue not only for its qualitative and quantitative economic implications but also from an econometric perspective. When concerned about the estimation of the structural parameters of the model, the econometrician will be interested in studying the global shape of the approximated likelihood function. This will not be possible if the solution of the model is built from a local approximation. Furthermore, as shown in Rubio-Ramírez and Fernández-Villaverde (2005), it is possible to obtain a better fit of the model to the data as well as more accurate point estimates of the moments of the model by exploiting the non-linear structure of the economic model, which can only be achieved through

the use of global methods. However, all these advantages come at a non-negligible cost. A good initial guess for the value function is required in order to obtain a good approximation that increases the computing time of the solution and hence compromises the feasibility of any econometric procedure.

On the other hand, the fit of perturbation and LQ approximations deteriorate when the degree of non-linearities is increased. In particular, they deliver approximated value and policy functions with a different level to that obtained by global methods. It has been argued previously in the literature that this could be explained by the lack of volatility correction implied by the certainty equivalence property. However, as mentioned in this paper, perturbation methods do not exhibit this property in the continuous-time framework and the same results are still obtained. A future line of research should include the study of this result more deeply.

From an econometric point of view, the use of perturbations is usually preferred since it makes the estimation of the deep parameters of the model simple and fast. However, as described in Fernández-Villaverde et al. (2006), the approximation error arising from the solution modifies the likelihood function. Ackerberg et al. (2009) have shown from a classical perspective that as the sample size increases the convergence of the parameters of interest to the true parameter vector is bounded by a term that is of the same magnitude as the approximation error made in the solution of the model. In addition, the period by period error made in the approximation accumulates at a rate exactly equal to the rate at which the sample size grows, making the approximated likelihood diverge from the exact likelihood. One way to circumvent these problems is to increase the order of the approximation in the solution step that comes at a very low computational cost, provided that such approximation remain within the radius of convergence.

Finally, after gathering the computing times of each of the numerical methods, I find that continuous-time DSGE modeling proves to be a promising area of future research when compared to the discrete-time framework. The approximation methods use much less computing time in both perturbation and projection methods since there is no need to approximate composition of unknown functions, neither to numerically approximate the integrals associated with expected values.

NOTES

1. Although the findings reported in this article are model dependent, they help to understand the different approximation methods, and a priori should carry over to other models.

2. A formal derivation of the HJB equation can be found in Chang (2009).

3. As mentioned in Judd (1998), the stable path corresponds to the root of the Ricatti equation that ensures concavity of the value function at the deterministic steady state. In other words, pick the $\mathcal{P}_i^{ss,0}$ compatible with $V_{ii}^{ss,0} < 0$. If all the roots fulfill this condition, then it is not possible to proceed due to the existence of indeterminacies in the economic model.

4. The family of multivariate polynomials generated by tensor products has the disadvantage of growing exponentially with the dimension of the state-space. One way to overcome this problem is to use the complete set of polynomials as discussed in Judd (1998) and Heer and Maussner (2009).

https://doi.org/10.1017/S1365100516000821 Published online by Cambridge University Press

5. A third type of projection called Garlekin projection is sometimes used in the literature. However, I do not treat it here since it usually delivers an approximation similar to that of least squares. Furthermore, by focusing only on collocation and least square projections I cover, from a more technical point, both orthogonal and non-orthogonal residual functions respectively as explained in McGrattan (2004).

6. The tolerance level for the iterative algorithms is fixed at $\mathcal{E} = 1.4901e^{-8}$.

7. Note that the perturbation method outperforms the projection method for the case of the labor supply. This is due to the fact that for the solution under Proposition 3.1, labor supply is constant but still its approximation depends on the approximation of a highly non-linear value function through equation (11).

8. See Cox et al. (1985) for a derivation of this formula.

9. In the discrete-time literature it is common to use as "true solution" the approximation obtained by value function iteration due to its convergence properties.

10. Alternative accuracy checks like the one proposed in Den Haan and Marcet (1994), or the simulation based assessments used in Taylor and Uhlig (1990) and Aruoba et al. (2006), are not used in this paper due to their discrete-time nature. Their implementation require a discretization procedure for the partial/stochastic differential equations that describe the model adding more errors to those already obtained in the approximation stage of the value and policy functions.

11. For projection methods, this measure is computed for the interpolated value and policy functions and not for the functions at the approximation nodes.

12. To prevent for under- and over-flow problems, the measure is corrected by computing its base 10 logarithm and adding a small number, respectively.

13. Simple simulations show that the time paths generated by the models with all the alternative calibrations are nonexplosive, and hence, perturbation methods remain valid approximations even for high degrees on nonlinearities.

14. To compute the approximations when no closed form is available, I follow the rule-of-thumb described in Section 4.2. However, it is important to keep in mind that this rule favors the collocation method over least squares since more time is used in the latter in order to find a good initial candidate for the former.

REFERENCES

Achdou, Y., Buera, F.J., Lasry, J.M., Lions, P.L., and Moll, B. (2014) Partial differential equation models in macroeconomics. *Philosophical Transactions of the Royal Society* A 372, 20130397.

Ackerberg, D., Geweke, J., and Hahn, J. (2009) Comments on "convergence properties of the likelihood of computed dynamic models". *Econometrica* 77(6), 2009–2017.

Aldrich, E. M. and Kung, H. (2010) Computational Methods for Production-Based Asset Pricing Models with Recursive Utility. Working papers 10-90, Duke University, Department of Economics.

Anderson, E. W., McGrattan, E. R., Hansen, L. P., and Sargent, T. J. (1996) Mechanics of forming and estimating dynamic linear economies. In H. M. Amman, D. A. Kendrick, and J. Rust (eds.), *Handbook of Computational Economics*, vol. 1, chap. 4, pp 171–252. Netherlands: Elsevier.

Aruoba, S. B., Fernández-Villaverde, J., and Rubio-Ramírez, J. F. (2006) Comparing solution methods for dynamic equilibrium economies. *Journal of Economic Dynamics and Control* 30(12), 2477–2508.

Benigno, P. and Woodford, M. (2012) Linear-quadratic approximation of optimal policy problems. *Journal of Economic Theory* 147(1), 1–42.

Bergstrom, A. (1984) Continuous time stochastic models and issues of aggregation over time. In Z. Griliches and M. D. Intriligator (eds.), *Handbook of Econometrics*, vol. 2, chap. 20, 1145–1212, Netherlands: Elsevier.

Binsbergen, J. v., Fernández-Villaverde, J., Koijen, R. S., and Rubio-Ramírez, J. (2012) The term structure of interest rates in a DSGE model with recursive preferences. *Journal of Monetary Economics* 59(7), 634–648.

Blanchard, O. (2009) The state of macro. *Annual Review of Economics* 1(1), 209–228.
Brennan, M. J. (1998) The role of learning in dynamic portfolio decisions. *European Finance Review* 1(3), 295–306.
Brunnermeier, M. K. and Sannikov, Y. (2014) A macroeconomic model with a financial sector. *American Economic Review* 104(2), 379–421.
Caldara, D., Fernández-Villaverde, J., Rubio-Ramírez, J., and Yao, W. (2012) Computing DSGE models with recursive preferences and stochastic volatility. *Review of Economic Dynamics* 15(2), 188–206.
Candler, G. V. (2004) Finite difference methods for continuous time dynamic programming. In R. Marimon and A. Scott (eds.), *Computational Methods for the Study of Dynamic Economies*, chap. 8, pp. 172–194. Oxford, UK: Oxford University Press.
Chang, F. R. (2009) *Stochastic Optimization in Continuous Time*, 2nd ed. Cambridge, UK: Cambridge University Press.
Collard, F. and Juillard, M. (2001) Accuracy of stochastic perturbation methods: The case of asset pricing models. *Journal of Economic Dynamics and Control* 25(6–7), 979–999.
Den Haan, W. J. and De Wind, J. (2010) How Well-Behaved are Higher-Order Perturbation Solutions? DNB working papers 240, Netherlands Central Bank, Research Department.
Den Haan, W. J. and Marcet, A. (1994) Accuracy in simulations. *Review of Economic Studies* 61(1), 3–17.
Doraszelski, U. and Judd, K. L. (2012) Avoiding the curse of dimensionality in dynamic stochastic games. *Quantitative Economics* 3(1), 53–93.
Fernández-Villaverde, J., Rubio-Ramírez, J. F., and Santos, M. S. (2006) Convergence properties of the likelihood of computed dynamic models. *Econometrica* 74(1), 93–119.
Furlanetto, F. and Seneca, M. (2014) New perspectives on depreciation shocks as a source of business cycle fluctuations. *Macroeconomic Dynamics* 18, 1209–1233.
Gaspar, J. and Judd, K. (1997) Solving large-scale rational-expectations models. *Macroeconomic Dynamics* 1(1), 45–75.
Gourio, F. (2012) Disaster risk and business cycles. *American Economic Review* 102(6), 2734–2766.
Grinols, E. L. and Turnovsky, S. J. (1993) Risk, the financial market, and macroeconomic equilibrium. *Journal of Economic Dynamics and Control* 17(1–2), 1–36.
Harvey, A. and Stock, J. H. (1989) Estimating integrated higher-order continuous time autoregressions with an application to money-income causality. *Journal of Econometrics* 42, 319–336.
Heer, B. and Maussner, A. (2009) *Dynamic General Equilibrium Modeling: Computational Methods and Applications*, 2nd ed. Heidelberg: Springer-Verlag.
Judd, K. L. (1996) Approximation, perturbation, and projection methods in economic analysis. In H. M. Amman, D. A. Kendrick, and J. Rust (eds.), *Handbook of Computational Economics*, vol. 1, chap. 12, pp. 509–585. Netherlands: Elsevier.
Judd, K. L. (1998) *Numerical Methods in Economics*. Cambridge, MA: MIT Press.
Judd, K. L. and Guu, S. M. (1993) Perturbation methods for economic growth models. In H. R. Varian (ed.), *Economic and Financial Modeling with Mathematica*, chap. 2, pp. 80–103. New York: Springer-Verlag.
Kimball, M. S. (2014) Effect of uncertainty on optimal control models in the neighbourhood of a steady state. *Geneva Risk Insurance Review* 39(1), 2–39.
Kompas, T. and Chu, L. (2012) A comparison of parametric approximation techniques to continuous-time stochastic dynamic programming problems: Applications to natural resource modelling. *Enviornmental Modelling and Software* 38, 1–12.
Kydland, F. E. and Prescott, E. C. (1982) Time to build and aggregate fluctuations. *Econometrica* 50(6), 1345–1370.
Ljungqvist, L. and Sargent, T. J. (2004) *Recursive Macroeconomic Theory*, 2nd ed. Cambridge, MA: MIT Press.
Magill, M. J. P. (1977a) Some new results on the local stability of the process of capital accumulation. *Journal of Economic Theory* 15(1), 174–210.

Magill, M. J. P. (1977b) A local analysis of n-sector capital accumulation under uncertainty. *Journal of Economic Theory* 15(1), 211–219.
McCandless, G. (2008) *The ABCs of RBCs: An Introduction to Dynamic Macroeconomic Models*. Cambridge, MA: Harvard University Press.
McGrattan, E. (2004) Application of weighted residual methods to dynamic economic models. In R. Marimon and A. Scott (eds.), *Computational Methods for the Study of Dynamic Economies*, chap. 6, pp. 114–142. Oxford, UK: Oxford University Press.
Miranda, M. J. and Fackler, P. L. (2002) *Applied Computational Economics and Finance*. Cambridge, MA: MIT Press.
Nuño, G. and Thomas, C. (2015) Monetary Policy and Sovereign Debt Vulnerability. Tech. rep., Banco de Espana. Unpublished.
Posch, O. (2011) Risk premia in general equilibrium. *Journal of Economic Dynamics and Control* 35(9), 1557–1576.
Posch, O. and Trimborn, T. (2013) Numerical solution of dynamic equilibrium models under poisson uncertainty. *Journal of Economic Dynamics and Control* 37(12), 2602–2622.
Rubio-Ramírez, J. F. and Fernández-Villaverde, J. (2005) Estimating dynamic equilibrium economies: Linear versus nonlinear likelihood. *Journal of Applied Econometrics* 20(7), 891–910.
Stokey, N. L. (2009) *The Economics of Inaction*. New Jersey: Princeton University Press.
Swanson, E. T. (2012) Risk aversion and the labor margin in dynamic equilibrium models. *American Economic Review* 102(4), 1663–1691.
Tapiero, C. S. and Sulem, A. (1994) Computational aspects in applied stochastic control. *Computational Economics* 7(2), 109–146.
Taylor, J. B. and Uhlig, H. (1990) Solving nonlinear stochastic growth models: A comparison of alternative solution methods. *Journal of Business & Economic Statistics* 8(1), 1–17.
Turnovsky, S. J. and Smith, W. T. (2006) Equilibrium consumption and precautionary savings in a stochastically growing economy. *Journal of Economic Dynamics and Control* 30(2), 243–278.
Wachter, J. (2013) Can time-varying risk of rare disasters explain aggregate stock market volatility? *Journal of Finance* 68(3), 987–1035.
Wälde, K. (2011) Production technologies in stochastic continuous time models. *Journal of Economic Dynamics and Control* 35(4), 616–622.
Xia, Y. (2001) Learning about predictability: The effects of parameter uncertainty on dynamic asset allocation. *Journal of Finance* 56(1), 205–246.

APPENDIX

A.1. EQUIVALENT BENCHMARK MODEL

By using the aggregate resource constraint of the economy, $Y_t = C_t + I_t$, equations (5) and (7), the model described in Section 3 can be written in the following equivalent way:

$$V(K_0, A_0) \equiv \max_{\{I_t, L_t\}_{t=0}^{\infty}} \mathbf{E}_0 \int_0^{\infty} e^{-\rho t} \frac{\left(\left(A_t K_t^{\alpha} L_t^{1-\alpha} - I_t\right)(1-L_t)^{\psi}\right)^{1-\gamma}}{1-\gamma} dt,$$

subject to:

$$dK_t = (I_t - \delta K_t)\, dt + \sigma K_t dB_{K,t},$$
$$dA_t = \kappa(\omega - A_t)\, dt + \eta\sqrt{A_t} dB_{A,t},$$

https://doi.org/10.1017/S1365100516000821 Published online by Cambridge University Press

where now the control variables are the level of investment, I_t, and the fraction of hours worked, L_t. Note that under this alternative representation, the drift function of both stochastic state processes is linear in the control and state variables.

Once the model has been solved for their respective policy functions it is possible to recover the level of optimal consumption by using the aggregate resource constraint:

$$C_t = A_t K_t^{\alpha} L\left(K_t, A_t\right)^{1-\alpha} - I\left(K_t, A_t\right).$$

A.2. HJB RESIDUALS

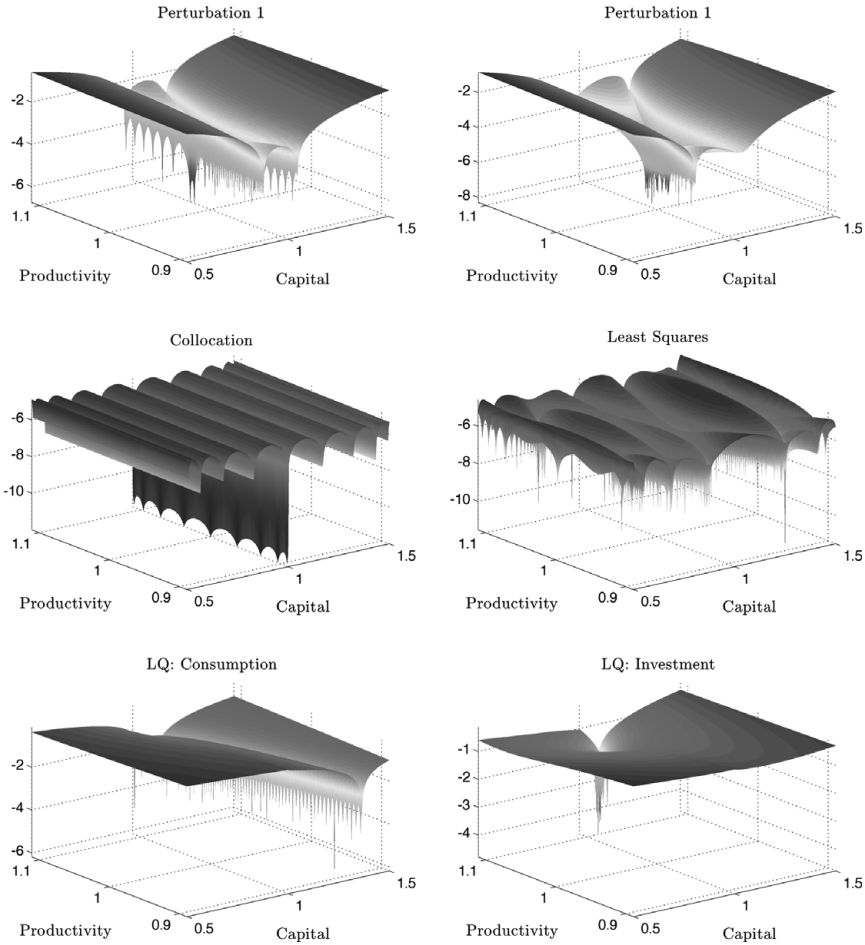

FIGURE A.1. HJB residuals K_t and A_t. The graph plots the HJB residuals under the benchmark calibration along the entire state space for the different approximation methods.

https://doi.org/10.1017/S1365100516000821 Published online by Cambridge University Press